Mathematical & Computational Applications, Vol. 5, No. 2, pp. 77-89, 2000

ELASTIC-PLASTIC STRESS ANALYSIS IN THERMOPLASTIC COMPOSITE CANTILEVER LOADED BY A SINGLE FORCE

R. ÖZCAN
Department of Mechanical Engineering, Uludağ University, Görükle, Bursa, Türkiye

Abstract- In this investigation an elastic-plastic stress analysis is carried out in a steel fiber reinforced thermoplastic composite cantilever. The beam is loaded by a single force at its free end. An analytical elastic-plastic solution is found by satisfying both equations of equilibrium and boundary conditions. Orientation angles are chosen as 0°, 30°, 45°, 60° and 90°. Yielding starts at upper or lower surfaces of the beam at different distances from the free end for 30°, 45°, 60° orientation angles. Maximum residual stresses are obtained at the upper and lower surfaces of the beam. For the shear stress, maximum stress component is found around the x-axis.

1. INTRODUCTION

Thermoplastic matrix composites are gaining popularity due to many high advantages. They offer high specific stiffness, and specific strength, improved interlaminar fracture toughness, increased impact resistance, and higher solvent resistance. In addition to their competitive mechanical properties, thermoplastic composites do not require complex chemical reactions to be processed and can be formed without lengthy curing processes. Experimental investigations on the forming of advanced thermoplastic composites can be found in References [1,2,3,4].

Residual stresses are particularly important in composites, because they can lead to premature failure. Jeronimidis *et al.* [5] obtained residual stress in carbon-fibre-thermoplastic matrix laminates. Owen *et al.* [6] carried out an elasto-plastic stress analysis of anisotropic plates and shells, undertaken by means of the finite element method. Domb *et al.* [7] developed a numerical model for prediction of the process induced thermal residual stress in thermoplastic composite laminates.

Chung *et al.* [8] used the same potential function as in the finite element method to obtain plastic flow and time-dependent creep deformation in thermoplastic composites.

Elasto-plastic stress analysis was carried out for the case of in-plane mechanical loading [9]. Finite element method is used to determine elasto-plastic stress in composite plates [10, 11, 12].

Karakuzu and Ozcan [13] carried out an elasto-plastic stress analysis in metal-matrix composite beam loaded uniformly or by a single force at the free end by using an analytical solution. In that solution they found the stress components by using static equilibrium.

In this study, an exact elasto-plastic stress analysis is carried out in a thermoplastic composite cantilever beam loaded at its free end by a single force. Stress components are determined by using equations of equilibrium and boundary conditions. Finally, residual stress components and the expansion of the plastic zone are obtained.

2. ELASTIC SOLUTION

In a plane stress problem, the governing differential equation is given by Lekhnitskii [14] as,

$$a_{22}\frac{\partial^4 F}{\partial x^4} - 2a_{26}\frac{\partial^4 F}{\partial x^3 \partial y} + (2a_{12} + a_{66})\frac{\partial^4 F}{\partial x^2 \partial y^2} - 2a_{16}\frac{\partial^4 F}{\partial x\ \partial y^3} + a_{11}\frac{\partial^4 F}{\partial y^4} = 0$$
(1)

where F is a stress function. The reduced stress-strain relationship for an orthotropic material is given as [15],

$$\begin{vmatrix} \varepsilon_x \\ \varepsilon_y \\ \gamma_{xy} \end{vmatrix} = \begin{vmatrix} a_{11} & a_{12} & a_{16} \\ a_{21} & a_{22} & a_{26} \\ a_{16} & a_{26} & a_{66} \end{vmatrix} . \begin{vmatrix} \sigma_x \\ \sigma_y \\ \tau_{xy} \end{vmatrix} \tag{2}$$

where a_{ij} are the components of compliance matrix as,

$$\begin{aligned} a_{11} &= S_{11}m^4 + (2S_{12} + S_{66})m^2n^2 + S_{22}n^4 \\ a_{12} &= S_{12}(m^4 + n^4) + (S_{11} + S_{22} - S_{66})m^2n^2 \\ a_{22} &= S_{11}n^4 + (2S_{12} + S_{66})m^2n^2 + S_{22}m^4 \\ a_{16} &= (2S_{11} - 2S_{12} - S_{66})nm^3 - (2S_{22} - 2S_{12} - S_{66})n^3m \\ a_{26} &= (2S_{11} - 2S_{12} - S_{66})n^3m - (2S_{22} - 2S_{12} - S_{66})nm^3 \\ a_{66} &= 2(2S_{11} + 2S_{22} - 4S_{12} - S_{66})m^2n^2 + S_{66}(m^4 + n^4) \end{aligned} \tag{3}$$

where $m = \text{Cos}\theta$, $n = \text{Sin}\theta$, $S_{11}=1/E_1$, $S_{22}=1/E_2$, $S_{12}=-\nu_{12}/E_1$, $S_{66}=1/G_{12}$.
A polynominal chosen for the solution of the governing differential equation (1) is given as:

$$F = \frac{d}{6}xy^3 + \frac{e}{12}y^4 + \frac{a}{2}y^2 + bxy \tag{4}$$

Placing in the equation (1) gives,

$$-2a_{16}d + a_{11}2e = 0 \tag{5}$$

from this equation e is found as,

$$e = rd \tag{6}$$

where $r = a_{16} / a_{11}$. The stress components for a plane problem are obtained from the stress function as;

$$\begin{aligned} \sigma_x &= dxy + rdy^2 + a \\ \sigma_y &= 0 \\ \tau_{xy} &= -\frac{d}{2}y^2 - b \end{aligned} \tag{7}$$

Boundary conditions in this beam are written as, (as shown in Figure 1.)

$$
\begin{aligned}
&\tau_{xy} = 0 \qquad at \quad y = \pm c \\
&\int_{-c}^{c} \tau_{xy} t\, dy = -P \\
&\int_{-c}^{c} \sigma_x t\, dy = 0 \qquad at\ x = 0 \\
&\int_{-c}^{c} \sigma_x t\, y\, dy = 0 \qquad at\ x = 0
\end{aligned}
\tag{8}
$$

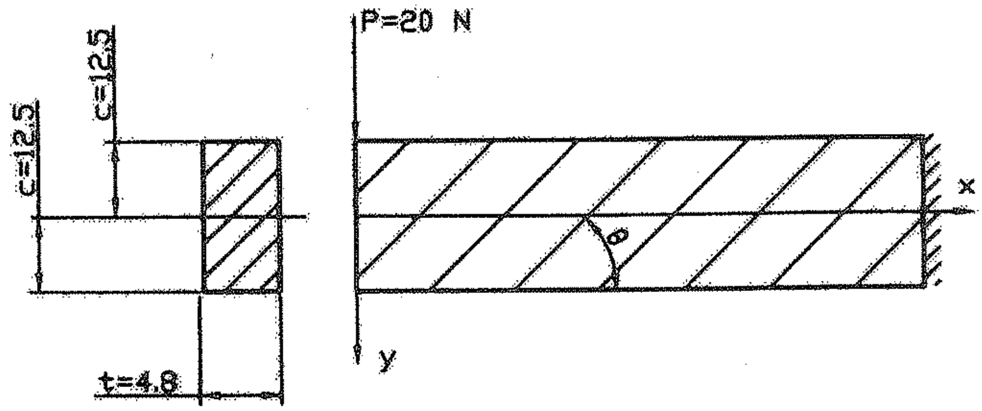

Figure 1. Composite cantilever loaded at its free end.

where t is the thickness of the beam. For satisfying the boundary conditions the unknown parameters are found as,

$$
b = -\frac{d}{2}c^2, \quad a = -r\frac{d}{3}c^2, \quad d = -\frac{P}{I} \tag{9}
$$

where I is the inertia moment of the cross section of the beam. Putting them in the stress components give

$$
\begin{aligned}
\sigma_x &= -\frac{P}{I}\left(xy + ry^2 - \frac{r}{3}c^2\right) \\
\sigma_y &= 0 \\
\tau_{xy} &= -\frac{P}{2I}\left(c^2 - y^2\right)
\end{aligned}
\tag{10}
$$

The stress components satisfy both the differential equation and all of the boundary conditions.

3. ELASTIC-PLASTIC SOLUTION

During the elastic-plastic stress analysis, it is assumed that the composite material is perfectly plastic. That is, strain hardening is neglected. The equations of equilibrium for a plane-stress case ignoring body forces are written as

$$\frac{\partial \sigma_x}{\partial x} + \frac{\partial \tau_{xy}}{\partial y} = 0$$
$$\frac{\partial \tau_{xy}}{\partial x} + \frac{\partial \sigma_y}{\partial y} = 0 \tag{11}$$

Substituting $\sigma_y = 0$ in the second equation gives $\tau_{xy} = f(y)$. Tsai-Hill theory is used as a yield criterion in this solution, it is given as,

$$\sigma_1^2 - \sigma_1\sigma_2 + \left(\frac{\sigma_2 X}{Y}\right)^2 + \left(\frac{\tau_{12} X}{S}\right)^2 = X^2 \tag{12}$$

where X and Y are the yield points of the composite beam in the principal material directions, 1 and 2, respectively. The yield point in the 3rd principal material direction is assumed to be equal to Y in the 2 direction because of the same alignment of the fibers in these directions. S is the yield point in a pure shear test. By using the transformation formula, stress components in the principal material directions are written as:

$$\sigma_1 = \sigma_x \cos^2\theta + 2\tau_{xy} \sin\theta \ \cos\theta$$
$$\sigma_2 = \sigma_x \sin^2\theta - 2\tau_{xy} \sin\theta \ \cos\theta \tag{13}$$
$$\tau_{12} = -\sigma_x \sin\theta \ \cos\theta + \tau_{xy}\left(\cos^2\theta - \sin^2\theta\right)$$

By using $\frac{\partial \tau_{xy}}{\partial x} = 0$ and the derivation of the Equation (12) with respect to x gives $\frac{\partial \sigma_x}{\partial x} = 0$. Putting this in the first differential Equation (11) gives that τ_{xy} is a constant or zero. But yielding begins at the upper or lower surfaces of the beam. It is also known that τ_{xy} is zero at those surfaces. Therefore, in the plastic zone τ_{xy} is equal to zero and σ_x is a constant. For an orientation angle θ, the stress component σ_x causes the material to yield for a perfectly plastic material it is found as,

$$\sigma_x = X_1 = \frac{X}{\sqrt{\cos^4\theta - \sin^2\theta\cos^2\theta + \frac{X^2\sin^4\theta}{Y^2} + \frac{X^2\sin^2\theta\cos^2\theta}{S^2}}} \tag{14}$$

In the plastic zone σ_x and τ_{xy} are equal to X_1 and zero, respectively.
During the elastic-plastic solution of the thermoplastic beam, the beam is divided into two parts, as seen in Figure 2.

For a general case, the yielding begins at the upper and lower surfaces at different distances. Yielding usually starts at the upper surfaces earlier than that at the lower surface.

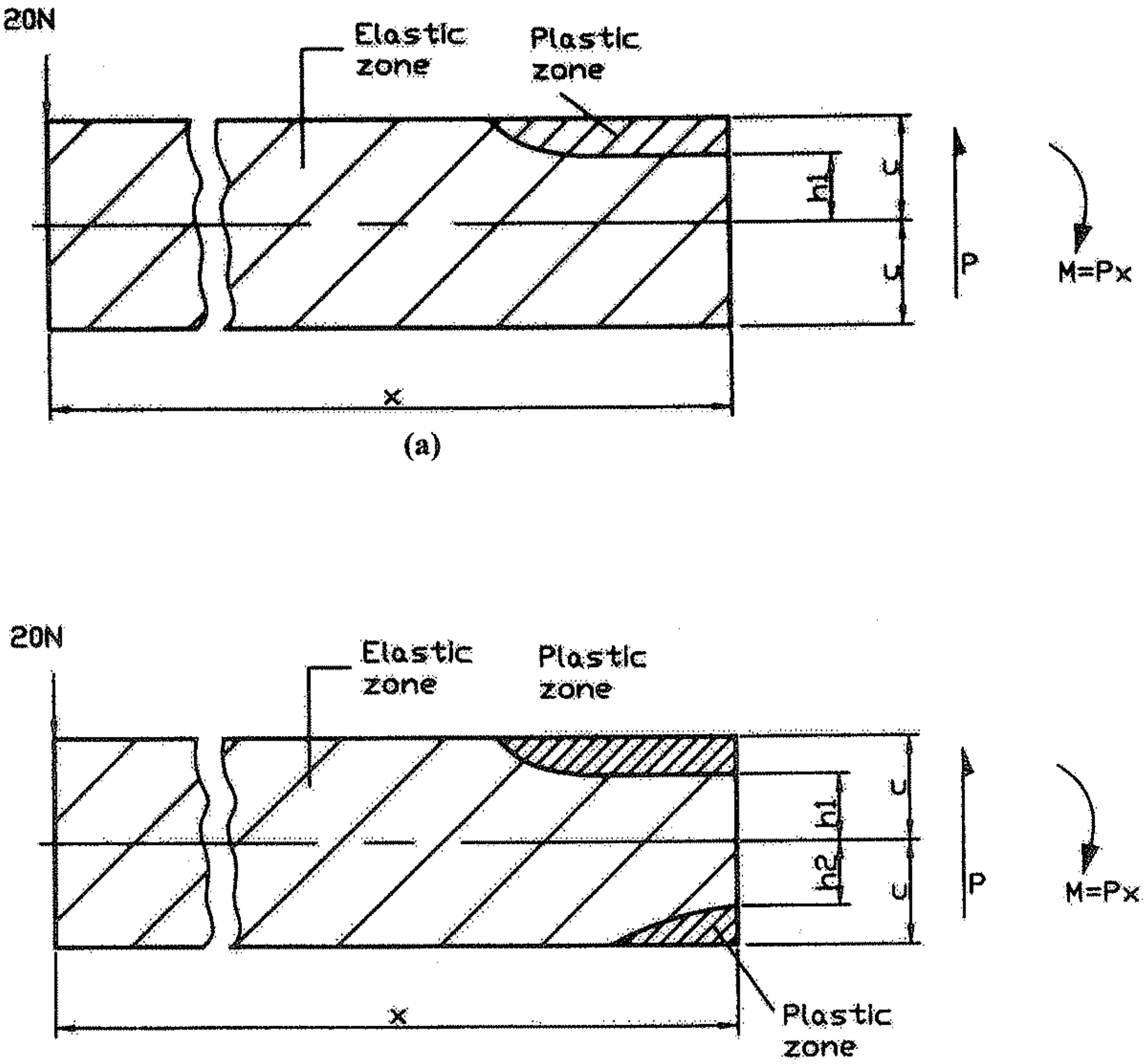

(b)

Figure 2. Elastic-plastic zones.

Part I. It is shown in Figure 2a, the boundary conditions are given as,

$$\begin{aligned} &\tau_{xy} = 0 \qquad at \quad y = -h_1 \\ &\int_{-h_1}^{c} \tau_{xy}\, t\, dy = -P \\ &\sigma_x = X_1 \qquad at \quad y = -h_1 \end{aligned} \tag{15}$$

where t is the thickness of the beam, and the resultant of σ_x across the cross section is zero.

$$X_1(c - h_1)t + \int_{-h_1}^{c} \sigma_x t dy = 0$$

also the moment of σ_x, across the cross section is equal to bending moment as,

$$\frac{X_1(c-h_1)t(c+h_1)}{2}-\int_{-h_1}^{c}\sigma_x t\, y\, dy=M=Px$$

Positive σ_x gives a negative moment, therefore the integration has a negative sign. The stress function is chosen to satisfy both the boundary conditions and governing differential equation as,

$$F=\frac{d}{6}xy^3+\frac{e}{12}y^4+\frac{a}{2}y^2+\frac{f}{6}y^3+\frac{k}{2}xy^2+bxy \tag{16}$$

Stress components for this stress function are,

$$\begin{aligned}\sigma_x&=dxy+rdy^2+fy+kx+a\\ \sigma_y&=0\\ \tau_{xy}&=-\frac{d}{2}y^2-ky-b\end{aligned} \tag{17}$$

where $r = a_{16} / a_{11}$. The constants are found from the boundary conditions as,

$$k=\frac{d(h_1-c)}{2},\qquad b=-\frac{dh_1c}{2},\qquad d=-\frac{P}{\dfrac{t(c+h_1)^3}{12}}$$

$$\begin{aligned}f&=-\frac{4cX_1}{(c+h_1)^2}-dx-\frac{2rd}{3}(c-2h_1)\\ a&=X_1+\frac{dx(h_1+c)}{2}+fh_1-rdh_1^{\,2}\end{aligned} \tag{18}$$

and

$$h_1=\frac{P(3x-cr)-4X_1c^2t}{rP-2X_1ct}$$

The solution of the last equation gives h_1 and subsequently the other parameters can be calculated.

Part II. In this part (As shown in Figure 2b), plastic zone expands both at the upper and lower surfaces. The boundary conditions in this region are given as,

$$\begin{aligned}&\tau_{xy}=0 \quad at \quad y=-h_1\\ &\tau_{xy}=0 \quad at \quad y=h_2\\ &\int_{-h_1}^{h_2}\tau_{xy}t\;dy=-P\\ &\sigma_x=X_1 \quad at \quad y=-h_1\\ &\sigma_x=-X_1 \quad at \quad y=h_2\end{aligned} \tag{19}$$

The resultant of σ_x along the cross section is equal to zero as;

$$X_1 t \ (c-h_1) - X_1 t(c-h_2) + \int_{-h_1}^{h_2} \sigma_x t dy = 0$$

The moment of σ_x along the cross section is equal to Px as;

$$\frac{X_1 t \ (c^2 - h_1^2)}{2} + \frac{X_1 t \ (c^2 - h_2^2)}{2} - \int_{-h_1}^{h_2} \sigma_x t y dy = Px$$

The stress function is chosen as to satisfy both the governing differential equation (1) and the boundary conditions as,

$$F = \frac{d}{6} xy^3 + \frac{e}{12} y^4 + \frac{a}{2} y^2 + \frac{f}{6} y^3 + \frac{k}{2} xy^2 + bxy \tag{20}$$

Stress components are obtained from this stress function as,

$$\begin{aligned} \sigma_x &= dxy + rdy^2 + fy + kx + a \\ \sigma_y &= 0 \\ \tau_{xy} &= -\frac{d}{2} y^2 - ky - b \end{aligned} \tag{21}$$

where r = a_{16} / a_{11}. From the boundary conditions the unknown seven parameters are found as

$$k = \frac{d(h_1 - h_2)}{2}, \qquad b = -\frac{dh_1 h_2}{2}, \qquad d = -\frac{12P}{t(h_1 + h_2)^3}$$

$$\begin{aligned} f &= \frac{rd(h_1^2 - h_2^2) - dx(h_1 + h_2) - 2X_1}{h_1 + h_2} \\ a &= -rdh_1 h_2 - \frac{X_1(h_1 - h_2)}{h_1 + h_2} - \frac{dx(h_1 - h_2)}{2} \\ h_2 &= h_1 - \frac{2\Pr}{X_1 t} \\ h_1 &= \frac{\frac{\Pr}{3t} + \sqrt{\frac{P^2 r^2}{3t^2} + \frac{c^2 X_1^2}{3} - \frac{PxX_1}{3}}}{\frac{X_1}{3}} \end{aligned} \tag{22}$$

From the last relation h_1 can be calculated and subsequently the other constants can be determined, easily.

4. PRODUCTION OF THE COMPOSITE BEAM

The thermoplastic composite material consists of low density polyethylene as a thermoplastic matrix and steel fibers. The raw material of the polyethylene is put into the moulds and the temperature is increased up to 160°C by using electrical resistance. Then the material is held for five minutes under 2.5 MPa pressure at this temperature. The temperature is decreased to 30°C under 15 MPa pressure in three minutes. Steel fibers are then placed between the two polyethylene layers and processed in the same way defined above, as shown in Figure 3. Mechanical properties and yield points of the composite layer are given in Table 1. The beam material is manufactured with the same procedure by using two composite layers bonded together. The thickness of the beam is produced as 4.8 mm.

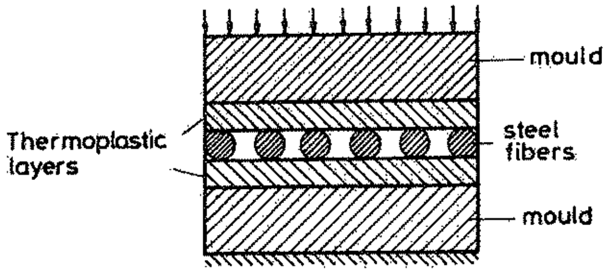

Figure 3. Production of a composite layer

Table 1. The measured mechanical properties and yield points of a layer.

Mechanical properties.

E_1	4300 MPa
E_2	960 MPa
G_{12}	240 MPa
ν_{12}	0.4

Yield strengths.

Axial Strength	X	21.0 MPa
Transverse Strength	Y	5.2 MPa
Shear Strength	S	5.8 MPa

5. RESULTS AND DISCUSSIONS

The cantilever beam is loaded by a load of 20 N at its free end. Points at which plastic yielding begins at the upper and lower surfaces from the free end are given at Table 2. It is seen from this Table that when the orientation angle is increased, the distance between the yield point and the free end becomes smaller. The first yield points at the upper and lower surfaces are at the same distances for 0° and 90° orientation angles. However, the distance between the yields points at the upper surface and the free end is smaller than that at the lower surface for 30° and 45° orientation angles. The yield points from the free end for the beam of 30° orientation angle are 259.20 mm and 275.76 mm at the upper and lower surfaces, respectively.

Table 2. First yield points at the upper and lower surfaces.

	Orientation angles				
	0°	30°	45°	60°	90°
First yield point at the upper surface (mm)	525.00	259.20	191.02	156.23	130.00
First yield point at the lower surface (mm)	525.00	275.76	196.15	153.31	130.00

5.1. Elastic-Plastic Stresses in Part I.

The plastic zone is thin in this part. It expands first at the upper surfaces for 30° and 45° orientation angles. The residual stress component of σ_x and the expansion of the plastic zone at the upper surface are given in Table 3. For the orientation angle of 60°, yielding starts first at the lower surface of the beam.

Table 3. Residual stress component and expansion of the plastic zone for 30° and 45° orientation angles.

Orientation Angle	Distance from the free end (mm)	h_1 (mm)	h_2 (mm)	(σ_x) residual at upper surface [MPa]
30°	259.20	12.50	12.50	0.00
	263.34	12.31	12.50	-0.17
	267.48	12.12	12.50	-0.33
	271.62	11.93	12.50	-0.50
45°	191.02	12.50	12.50	0.00
	192.30	12.42	12.50	-0.05
	193.59	12.34	12.50	-0.10
	194.87	12.25	12.50	-0.15

In this case, the distance between the x axis and the plastic zone is found as;

$$h_2 = \frac{-P(3x+cr)+4X_1tc^2}{rP+2X_1ct} \tag{23}$$

The residual stress component and the expansion of the plastic zone is illustrated in Table 4. It is seen from this table that when the distance from the free end is increased the plastic zone spreads only at the upper or lower surfaces.

Table 4. Residual stress component and the expansion of plastic zone for 60° orientation angle.

Orientation Angle	Distance from the free end (mm)	h_1 (mm)	h_2 (mm)	(σ_x) residual at the lower surface [MPa]
60°	153.31	12.50	12.50	0.00
	154.04	12.50	12.44	0.04
	154.77	12.50	12.38	0.08
	155.50	12.50	12.32	0.12

5.2 Elastic-Plastic Stresses in Part II.

In this case, the plastic zone expands both at the upper and lower surfaces. The expansion of the plastic zone and σ_x are given for all the orientation angles in Table 5. As seen from this Table, the plastic zone expands the same at the upper and lower surfaces for 0° and 90° orientation angles. It spreads at the upper surfaces more than that at the lower surfaces for 30° and 45° orientation angles; however, it spreads more at the lower surfaces for 60° orientation angle.

Table 5. Expansion of plastic zone and residual stress components (MPa) at the upper and lower surfaces.

	x (mm)	h_1 (mm)	h_2 (mm)	$(\sigma_x)_p$ at upper surface	$(\sigma_x)_p$ at lower surface	$(\sigma_x)_e$ at upper surface	$(\sigma_x)_e$ at lower surface	$(\sigma_x)_r$ at upper surface	$(\sigma_x)_r$ at lower surface
0°	530	12.38	12.38	21.00	-21.00-	21.20	-21.20	-0.20	0.20
	540	12.14	12.14	21.00	21.00	21.60	-21.60	-0.60	0.60
	550	11.89	11.89	21.00	-21.00	22.00	-22.00	-1.00	1.00
	560	11.64	11.64	21.00	-21.00	22.40	-22.40	-1.40	1.40
30°	280	11.52	12.29	10.67	-10.67	11.50	-10.84	-0.83	0.17
	290	11.02	11.79	10.67	-10.67	11.90	-11.24	-1.23	0.57
	300	10.49	11.27	10.67	-10.67	12.30	-11.64	-1.63	0.97
	310	9.94	10.72	10.67	-10.67	12.70	-12.04	-2.03	1.37
45°	200	11.91	12.25	7.74	-7.74	8.10	-7.89	-0.36	0.15
	210	11.23	11.56	7.74	-7.74	8.50	-8.29	-0.76	0.55
	220	10.49	10.83	7.74	-7.74	8.90	-8.69	-1.16	0.95
	230	9.71	10.04	7.74	-7.74	9.30	-9.09	-1.56	1.35
60°	160	12.19	11.95	6.19	-6.19	6.34	-6.46	-0.15	0.27
	170	11.32	11.09	6.19	-6.19	6.74	-6.86	-0.55	0.67
	180	10.38	10.14	6.19	-6.19	7.14	-7.26	-0.95	1.07
	190	9.34	9.11	6.19	-6.19	7.54	-7.66	-1.35	1.47

The distribution of the residual stress component of σ_x for the beam of 0° orientation angle is shown in Figure 4. As seen from this Figure the intensity of the residual stress component of σ_x is the same at the upper and lower surfaces. The distribution of the shear stress at the section of x = 590 mm is represented. Maximum residual stress component of τ_{xy} is found for any section at the x axis.

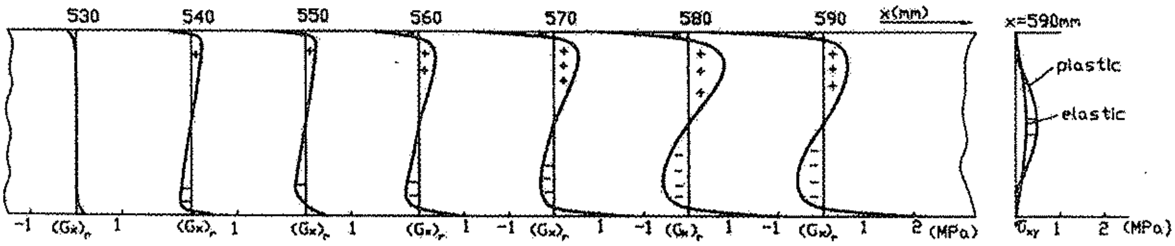

Figure 4. Distribution of the residual stress components for 0° orientation angle.

The distribution of the residual stress component of σ_x along the sections is shown in Figure 5 for the beam of 30° orientation angle. The intensity of the residual stress at the upper surface is greater than that at the lower surface. The intensity of the residual shear stress component is maximum at any section around the x axis.

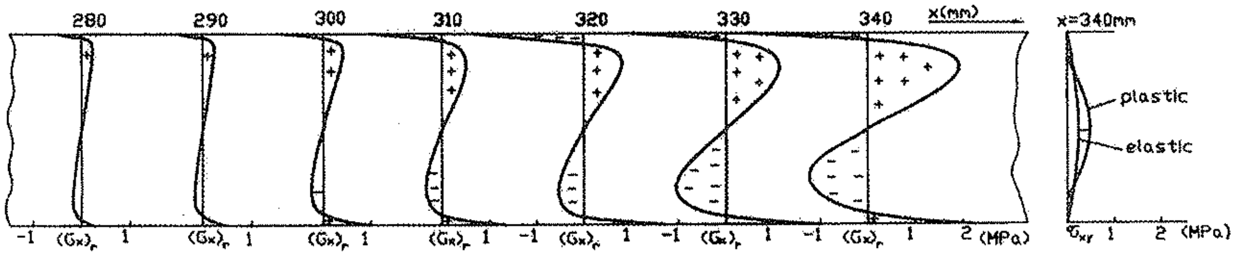

Figure 5. Distribution of the residual stress components for 30° orientation angle

The distribution of the residual stress component of σ_x and τ_{xy} for the 45° orientation angle is illustrated in Figure 6. As seen from this Figure that the intensity of the residual stress component of σ_x at the upper surface is greater than that for the lower surface. It is also seen that the plastic zone expands at the upper side larger than that at the lower side. The residual stress component of τ_{xy} of the distribution of the residual stress component of σ_x for the beam of 60° orientation angle is shown in Figure 7. As seen from this Figure, the intensity of the residual stress component at the lower surface is greater than at the upper surface. Again the residual stress component of τ_{xy} is maximum around the x axis.

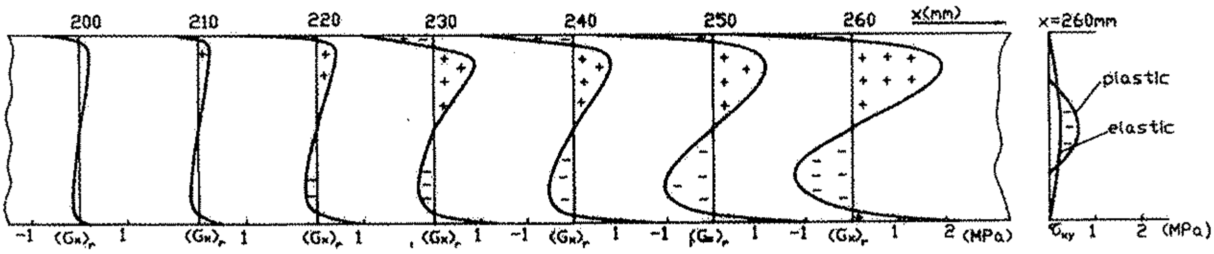

Figure 6. Distribution of the residual stress components for 45° orientation angle.

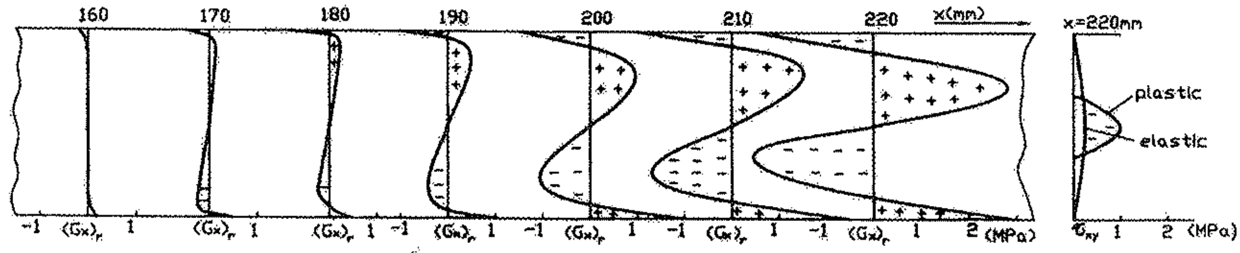

Figure 7. Distribution of the residual stress components for 60° orientation angle.

The distribution of the residual stress component of σ_x for the beam of 90° orientation angle is shown in Figure 8. The intensity of the residual stress components of σ_x and τ_{xy} is symmetric with respect to the x axis at any section. Plastic zone spreads rapidly in the beam of higher orientation angles.

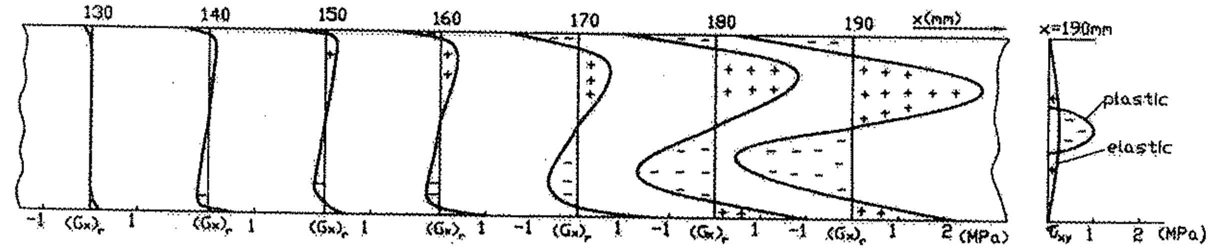

Figure 8. Distribution of the residual stress components for 90° orientation angle.

6. CONCLUSIONS

In the present study an exact solution is given for the elastic-plastic solution of a composite cantilever loaded at its free end by a single force.

1) The plastic zone starts first at the upper surfaces of the beam for 30° and 45° orientation angles. However, it begins earlier at the lower surface for 60° orientation angle also it expands at the same distances at the upper and lower surfaces for 0° and 90° orientation angles.
2) If the plastic zone expands at one of the upper and lower surfaces, the plastic zone is thin.
3) When the orientation angle is increased, the plastic zone spreads rapidly.
4) The intensity of the residual stress component of σ_x is maximum at the upper and lower surfaces.
5) The intensity of the residual stress component of τ_{xy} is maximum around the x axis.

REFERENCES

1. D. Jegley. Impact-damaged graphite-thermoplastic trapezoidal-corrugation sandwich and semi- sandwich panels, *Journal of Composite Materials*, 27, No.5, pp. 526-538, 1993.
2. C. H. Chen. And , C. H, Cheng, Secant moduli of a glass bead-reinforced silicone rubber specimen, *Journal of Composite Materials*, 30, No.1, pp. 69-83, 1996.
3. W. J. Cantwell. The influence of stamping temperature on the properties of a glass mat thermoplastic composite", *Journal of Composite Materials*, 30, No.11, pp. 1266-1281, 1996.
4. I. H. Tavman. Thermal and Mechanical Properties of Aliminum Powder Filled High Density Polyethylene Composites", *Journal of Applied Polymer Science*, 62, pp. 2161-2167, 1996.

5. G. Jeronimidis and A. T. Parkyn. Residual stress in carbon fibre- thermoplastic matrix laminates, *Journal of Composite Materials*, 22, No.5, pp. 401-415, 1998.
6. D. R. J. Owen and J. A. Figueiras. Anisotropic elasto-plastic finite element analysis of thick and thin plates and shells, *International Journal For Numerical Methods in Engineering*, 19, pp. 541-566, 1983.
7. M. M. Domb and J. S. Hansen. The effect of cooling rate on free-edge stress development in semi-crystalline thermoplastic laminates, *Journal of Composite Materials*, 32, No.4, pp. 361-385, 1998.
8. I. Chung, C. T. Sun and I. Y. Chang. Modelling creep in thermoplastic composites" , *Journal of Composite Materials*, 27, No.10, pp. 1009-1029, 1993.
9. Y. A. Bahei-El-Din and G. J. Dvorak. Plasticity analysis of laminated composite plates, *Transactions of the Asme*, 49, pp. 740-746, 1982.
10. R. Karakuzu and O. Sayman. Elasto-plastic finite element analysis of orthotropic rotating discs with holes, *Computers and Structures*, 51, No.6, pp. 695-703, 1994.
11. R. Karakuzu, A. Ozel and O. Sayman. Elasto-plastic finite element analysis of metal-matrix plates with edge notches, *Computers and Structures*, 63, No.3, pp. 551-558, 1997.
12. O. Sayman. Elasto-plastic stress analysis in stainless steel fiber reinforced aluminum metal matrix laminated plates loaded transversely, *Composite Structures*, 43, pp. 147-154, 1998.
13. R. Karakuzu and R. Ozcan. Exact solution of elasto-plastic stresses in a metal –matrix composite beam of arbitrary orientation subjected to transverse loads, *Composites Science and Technology*, 56, pp. 1383-1389, 1996.
14. S. G. Lekhnitskii. *Theory of Elasticity of an Anisotropic Body*, Mir Publishers, Moscow, 1981.
15. R. M. Jones. *Mechanics of Composite Materials*, McGraw-Hill Kogakuska, Tokyo, 1975.